CHAPTER III. SYNTHESIS OF THE BENZYLISOQUINOLINE ALKALOID BACKBONE FROM TYROSINE IN *SACCHAROMYCES CEREVISIAE*

Abstract

This work focuses on the development of a recombinant pathway for the production of the benzylisoquinoline alkaloid (BIA) backbone in *Saccharomyces cerevisiae*. The true intermediate in the native plant pathway is (*S*)-norcoclaurine but extensions of this engineered pathway can also use (*R, S*)-norlaudanosoline as a precursor. These simple BIAs are derived from two molecules of tyrosine which can be synthesized by yeast in addition to being a standard media component. We engineered numerous yeast strains to express heterologous and endogenous enzymes for the production of dopamine, 4-hydroxyphenylacetaldehyde (4-HPA), and 3,4-dihydroxyphenylacetaldehyde (3,4-DHPA) intermediates. While no single strain has been optimized to the point of achieving *de novo* biosynthesis of BIAs, these experiments laid the groundwork for producing these molecules from tyrosine in yeast. This upstream pathway can later be combined with downstream steps for the total biosynthesis of a variety of pharmacologically-relevant molecules.

3.1. Introduction

The benzylisoquinoline alkaloids (BIAs) are a large and diverse group of natural products with ~2,500 defined structures, including many with potent pharmacological properties[40]. The complex biosynthesis of BIAs in plants begins with the condensation of the backbone structure derived from two molecules of tyrosine. Along one branch, tyrosine is converted to dopamine and a second molecule of tyrosine is converted to 4-hydroxyphenylacetaldehyde (4-HPA) along a second branch. Dopamine is the precursor for the isoquinoline moiety while 4-HPA is incorporated into the benzyl component (Fig. 3.1). Despite extensive investigations of *Papaver somniferum*, *Eschscholzia californcia*, *Thalictrum flavum*, *Coptis japonica* and other BIA producing plants, only two enzymes have been isolated from these very early steps involved in BIA biosynthesis[6].

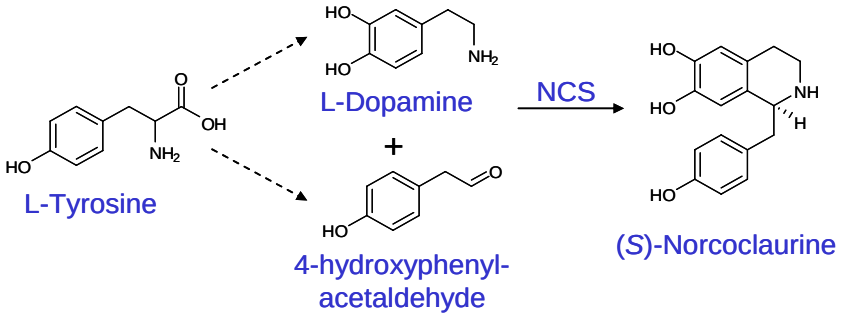

Fig. 3.1. The native pathway for the production of the BIA precursor (*S*)-norcoclaurine synthesized from two molecules of tyrosine.

The earliest enzyme cloned in this pathway is tyrosine decarboxylase (TYDC) which catalyzes the decarboxylation of tyrosine to tyramine or dihydroxyphenylalanine (L-dopa) to dopamine[41]. The other cloned enzyme in this upstream pathway is norcoclaurine synthase (NCS) which catalyzes the condensation of dopamine and 4-HPA, the first committed step in BIA biosynthesis. These enzymes can be incorporated into a

recombinant pathway but the remaining activities must be reconstituted using enzymes from other organisms. This work demonstrates the assembly of an engineered pathway in yeast that incorporates activities from plants, humans, bacteria, and fungi for the production of the BIA backbone molecule norcoclaurine and its analog norlaudanosoline.

3.2. Results

3.2.1. Functional expression of tyrosine/dopa decarboxylase from Papaver somniferum

Multiple gene sequences coding for tyrosine/dopa decarboxylase enzymes from *P. somniferum* have previously been cloned and characterized in *Escherichia coli*[41]. Yeast expression constructs for both TYDC1 and TYDC2 variants were made using a high-copy plasmid backbone and a strong promoter (TEF1). Initial experiments showed that TYDC2 outperformed TYDC1 *in vivo* in our yeast strains, with TYDC1 showing very little activity on tyrosine and L-dopa substrates (data not shown). This is somewhat unexpected given that previous results showed TYDC1 to have a higher specific activity for both substrates. However, kinetic data were gathered using fusion proteins with β-galactosidase which notably formed inclusion bodies in *E. coli* samples[41] and may not be directly transferable to yeast. We also noticed greater conversion of the substrate tyrosine compared to L-dopa, again contradicting *in vitro* results which suggest that the specific activity for tyrosine is only 65% of that of L-dopa. However, feeding an exogenous substrate can also introduce transport limitations, and tyrosine is more likely to be actively transported across yeast cell membranes. Moreover, results have shown that catecholamines including L-dopa and dopamine activate the yeast oxidative stress response pathway due to their ability to autooxidize. This is not only a source of loss of

these intermediates, but production of these molecules may impair growth and have other unintended effects. The similar compounds tyrosine and tyramine are more stable and do not elicit this response[42].

Results of *in vivo* assays using yeast cells constitutively expressing TYDC2 with tyrosine and L-dopa substrates added to the growth medium at a concentration of 1 mM are shown (Fig. 3.2). Tyramine production by TYDC2 in our engineered yeast strains is estimated to reach over 100 mg l^{-1} using standard yeast media and increases with the addition of exogenous tyrosine. Endogenous tyrosine biosynthesis can also influence the yield and may be a target for future metabolic engineering efforts.

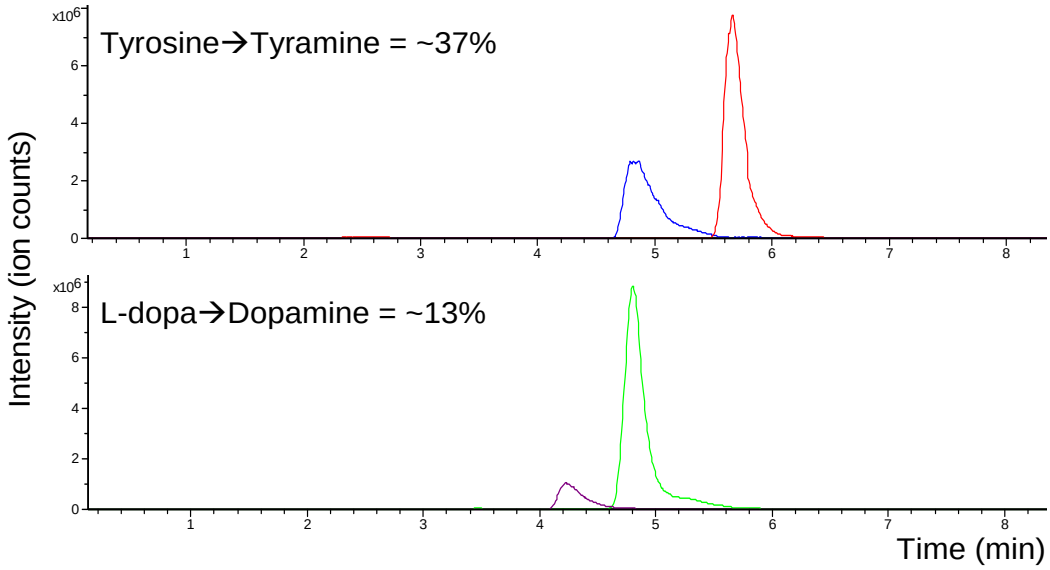

Fig. 3.2. *In vivo* TYDC2 assays. Top: LC-MS analysis of growth media of yeast strains expressing TYDC2 and supplemented with 1 mM tyrosine. Extracted ion chromatograms are shown for tyrosine (*m/z* = 182, red) and tyramine (*m/z* = 138, blue). Bottom: LC-MS analysis of growth media of yeast strains expressing TYDC2 and supplemented with 1 mM L-dopa. Extracted ion chromatograms are shown for L-dopa (*m/z* = 198, green) and dopamine (*m/z* = 154, purple). Percent conversion is calculated by the ratio of the peak areas.

3.2.2. Production of dopamine

Two different pathways for the production of dopamine that incorporate the TYDC2 activity are conceivable. One pathway requires a phenyloxidase activity to convert tyrosine to L-dopa while the other requires a phenolase activity to convert tyramine to dopamine (Fig. 3.3).

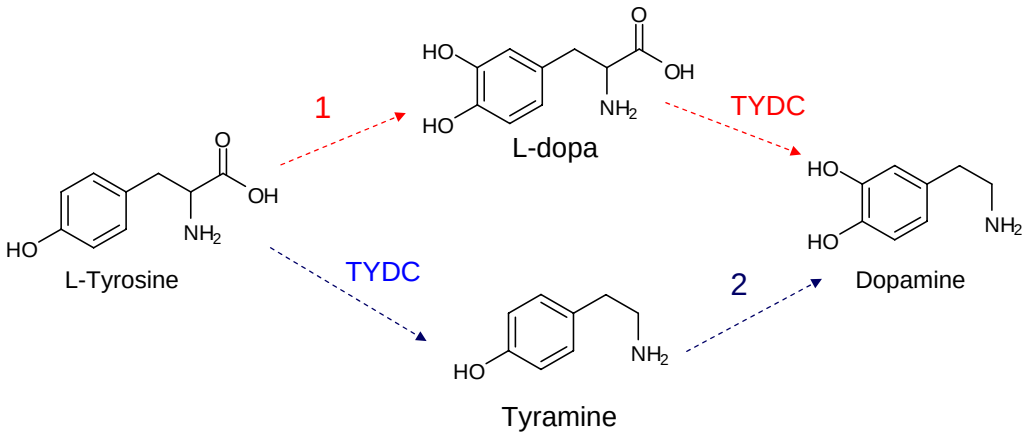

Fig. 3.3. Alternative pathways for dopamine production from tyrosine. The upper pathway (shown in red) uses an unnamed enzyme activity (1) to convert tyrosine to L-dopa and the TYDC activity to convert L-dopa to dopamine. The lower pathway (shown in blue) uses the TYDC activity to convert tyrosine to tyramine and a second enzyme activity (2) to convert tyramine to dopamine.

The oxidation of tyrosine to L-dopa can be catalyzed by three different types of enzymes: tyrosine hydroxylase, tyrosinase, and β-tyrosinase[43]. Tyrosinase activities are widely distributed in nature as they are key enzymes involved in melanin biosynthesis. However, in addition to catalyzing the orthohydroxylation of phenolic substrates, they also catalyze the oxidation of these catechol products to quinones. In the host organism and in the presence of activating nucleophiles, quinones are spontaneously polymerized to form melanin. Reactive quinone intermediates have antibiotic properties and melanin

itself exerts many strengthening and protective effects; however, accumulation of the L-dopa intermediate is desired in this case, contrary to what happens in nature.

Yeast strains were constructed to express either the human tyrosine hydroxylase 2 (hTH2) or rat tyrosine hydroxylase (TyrH) along with the human GTP cyclohydrolase I (hGTPCHI) required to synthesize the cofactor tetrahydrobiopterin (BH_4). Preliminary results indicated no L-dopa accumulation in the growth media or cell extracts of these strains. In addition, expression levels of these recombinant proteins were assayed by Western blotting using a standard epitope tag, and all three fell below the detection threshold. Difficulties with expression coupled to the fact that hTH2 in particular has a tyrosine hydroxylase to dopa oxidase ratio of ~2:1[44] led us to pursue other enzymes for this activity. However, methods such as codon-optimization, use of more favorable TH variants (such as hTH4), and optimization of the cofactors Cu(II) and BH_4 may show more encouraging results.

We also obtained sequences coding for two tyrosinase cDNAs from *Agaricus bisporus* (AbPPO1 and AbPPO2), the common button mushroom. Results from AbPPO2 expressed in yeast were encouraging but inconsistent. One strain was able to show production of dopamine when co-transformed with a plasmid expressing TYDC2. However, the addition of 1-10 μM $Cu(II)SO_4$, which should facilitate the catalytic activity of the copper-containing tyrosinase enzyme, increased accumulation of L-dopa but produced no dopamine. TYDC2 remained active in the presence of Cu(II) as evidenced by tyramine accumulation but failed to convert L-dopa to dopamine under these conditions (Fig. 3.4).

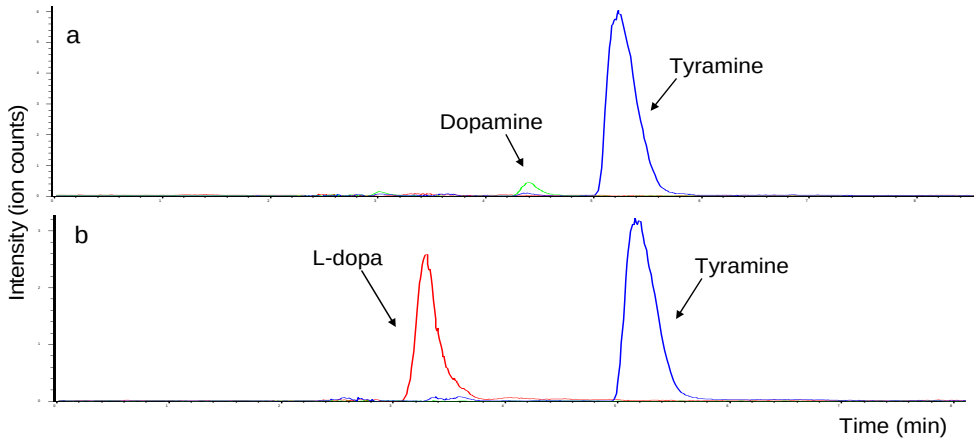

Fig. 3.4. LC-MS analysis of the growth media of CSY88 (Table 3.1) expressing AbPPO2 and TYDC2. **(a)** Production of tyramine (*m/z* = 138, blue) and dopamine (*m/z* = 154, green) are observed in synthetic complete media with no additives. **(b)** Production of tyramine (*m/z* = 138, blue) and L-dopa (*m/z* = 198) are observed when 5 μM Cu(II)SO_4 is added to the media; dopamine production is not detectable.

In an effort to increase metabolite shuttling between AbPPO2 and TYDC2 by co-localizing the enzymes *in vivo*, a fusion protein between the two enzymes was constructed and the proteins were tagged with matching C-terminal or N-terminal leucine zippers. In these strains, tyramine production remained high while L-dopa production was nearly abolished, and no dopamine was produced. As proteolytic processing of AbPPO2 in *Agaricus* is believed to take place from the C-terminal region[45], additional amino acids may interfere with processing and maturation of the protein. This is true specifically in the case of the fusion protein as it was constructed with the AbPPO2 domain on the N-terminus. Also, the C-terminal leucine zipper sequence would likely be cleaved during post-translational processing. Evidence for extensive proteolytic processing is provided by Western blotting analysis using N- and C-terminal tags (Fig. 3.5). However, the number of discrete bands suggests that the desired product does not dominate in our host. Differences in signal sequences and proteases between the two organisms may explain much of the lack of activity seen with our AbPPO2 constructs.

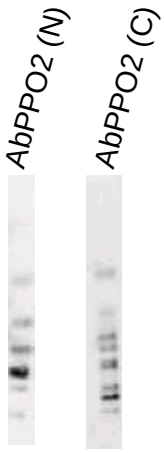

Fig. 3.5. Western blots of AbPPO2 constructs. Left: AbPPO2 with an N-terminal tag detected with an Anti-His G-HRP antibody. Right: AbPPO2 with a C-terminal tag detected with an Anti-V5 HRP antibody.

An alternative pathway for dopamine production proceeds through tyramine and requires the enzymatic addition of a 3'-hydroxyl group. The most well-characterized enzyme that performs this reaction is the human cytochrome P450 2D6 (hCYP2D6). While yeast is a suitable and often-used host for P450 expression, this class of enzymes still presents many difficulties as will be demonstrated throughout this work. Overexpression of the endogenous yeast NADPH cytochrome P450 reductase (yCPR1) or other heterologous P450 reductase is generally required to observe activity of P450 enzymes either *in vivo* or using yeast microsomal preparations. Among the most commonly used strains for expression of heterologous P450s are W(R) and WAT11 strains which contain genomic integrations of GAL-inducible yeast CPR1 and *Arabidopsis thaliana* ATR1 reductases, respectively[46]. We tested both strain backgrounds with co-expression of the TYDC2 and hCYP2D6 enzymes for dopamine production. The engineered yeast cells in the WAT11 strain background showed no dopamine production when grown in the presence of galactose, indicating that the *A. thaliana* ATR1 is not a

suitable reductase partner for hCYP2D6. The W(R) strain background produced dopamine, but surprisingly, no difference was observed between induced and uninduced cultures. This suggests that leaky expression of yCPR1 from the GAL1-10 promoter is sufficient to enhance the activity of its P450 partner above that seen in the wild-type background strain. Additional expression of the yCPR1 driven by the $tetO_2$ promoter (which is constitutive in the absence of doxycycline) further increased dopamine production. The use of rich media (2x yeast nitrogen base and 5 g l^{-1} casein hydrolysate instead of ammonium sulfate) also boosted dopamine production slightly but is not an economical solution for an industrial process.

We sought to improve CYP2D6 expression by optimizing codon usage of the gene for yeast. We were not able to observe either improved expression or activity but retained this sequence to reduce metabolic stress on the cells. We co-expressed this optimized sequence with the soluble yCPRΔ33 and also constructed a fusion protein between yCYP2D6 and yCPRΔ33. This fusion construct yielded the highest dopamine levels when expressed from a strong TEF6 promoter in a strain background with either an integrated or plasmid-based copy of TYDC2. This engineered yeast strain produced ~10 μM dopamine while other strains fell short of this mark (Fig. 3.6). Although experimental evidence suggests that this level should be sufficient for incorporation into norcoclaurine, we have not been able to demonstrate this *in vivo* by supplementing 4-HPA. Aside from the redox balance, many other factors may be limiting, including the low affinity of CYP2D6 for the substrate tyramine and autooxidation of dopamine. Additional protein evolution, strain engineering, and optimization of media conditions are required to address these potential issues.

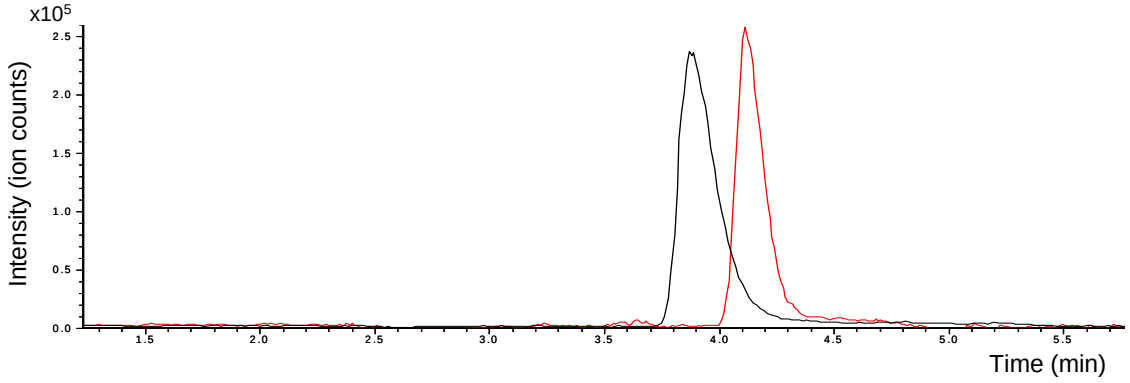

Fig. 3.6. LC-MS analysis of dopamine produced in yeast. Production of dopamine by engineered yeast strains expressing P_{TEF1}*:TYDC2* and P_{TEF6}*:yCYP2D6-yCPRΔ33* from high-copy plasmids (red; pCS221 and pCS1565) compared to a 10 μM dopamine standard (black). Extracted ion chromatograms for *m/z* = 154 are shown.

3.2.3. Production of 4-hydroxyphenylacetaldehyde and 3,4-dihydroxyphenylacetaldehyde

The other intermediate species required for norcoclaurine formation is 4-hydroxyphenylacetaldehyde (4-HPA). The characterization of this product is severely hindered by the lack of a commercially available standard. A small amount was synthesized (Bio Synthesis, Inc.) for use in downstream enzyme assays but was also very unstable in solution and difficult to detect by LC-MS due to the lack of a basic group for protonatization by electrospray ionization (ESI; Fig. 3.7). While this molecule is more amenable to UV detection, the absorbance of similar molecules in complex biological samples obstructs this type of analysis. Other detection methods such as thin-layer chromatography (TLC) and reaction with Purpald did not yield consistent and reliable results for our samples.

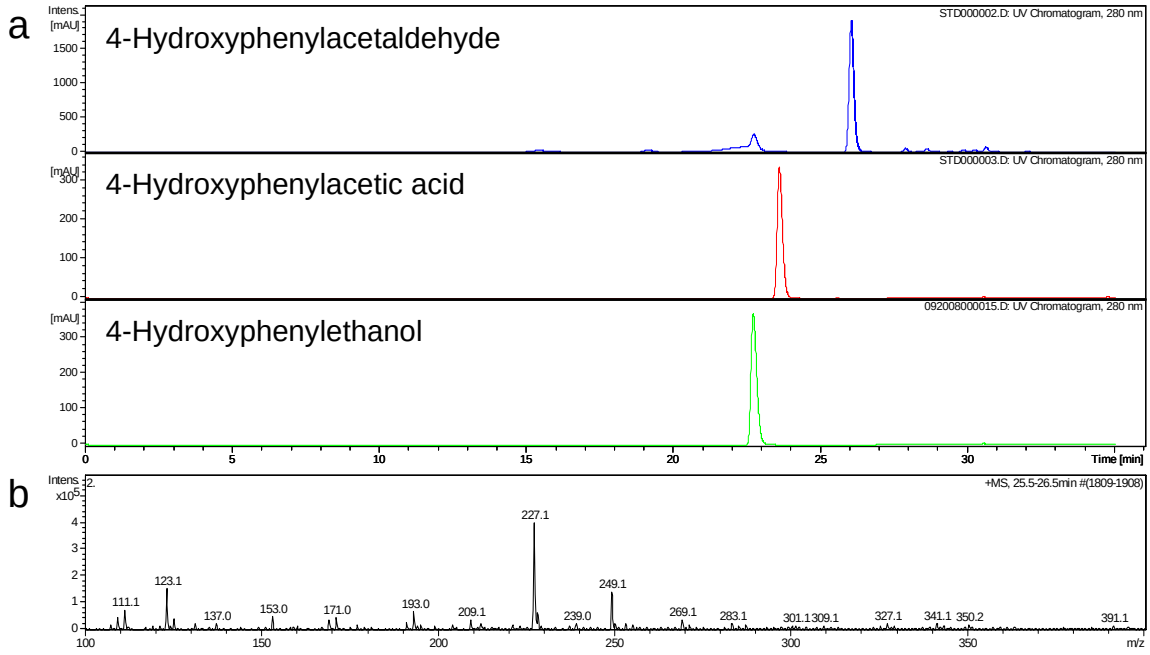

Fig. 3.7. Analysis of tyrosine derivatives. **(a)** LC-UV data of standards 4-HPA (blue; 26 min), 4-hydroxyphenylacetic acid (red; 23.5 min), and 4-hydroxyphenylethanol (green; 23.8 min). Absorbance is measured at a fixed wavelength of 280 nm. **(b)** The MS chromatogram of the 4-HPA peak at 26 min shows very low levels of the expected *m/z* = 137 ion. These small aromatic molecules lacking nitrogen are more amenable to UV detection than ESI-MS.

In addition to being chemically unstable, 4-HPA is also very enzymatically unstable *in vivo* similar to other reactive aldehyde species. We expect 4-HPA to be converted to either 4-hydroxyphenylacetic acid or 4-hydroxyphenylethanol (tyrosol) depending on the redox state of the cell. Tyrosol is one of the fusel alcohols produced via the Ehrlich pathway in yeast. Any one of five aldehyde dehydrogenase enzymes (*ALD2-6*) or seven alcohol dehydrogenase enzymes (*ADH1-7*) can potentially act on 4-HPA to divert this intermediate to central metabolism. For this reason, in many assays we sought to detect not only 4-HPA but other downstream products as well.

One possible pathway for 4-HPA production is the conversion of tyramine by a monoamine oxidase activity (Fig. 3.8a). These enzymes are ubiquitous in nature and we

constructed plasmids and yeast strains to test the *E. coli* monoamine oxidase (MaoA), the *Klebsiella aerogenes* W70 tyramine oxidase[47], the human liver monoamine oxidase (MAO-A) optimized for expression in yeast[48], and the *M. luteus* tyramine oxidase[49]. Initial experiments looking at protein expression levels and activity using a standard H_2O_2 assay eliminated the *K. aerogenes* tynA while the *E. coli* MaoA and human MAO-A were shown to be actively expressed in our yeast hosts (Fig. 3.8b). The *M. luteus* tyramine oxidase was later codon-optimized and assembled using short oligonucleotides based on its use in other microbial BIA pathway work[50].

To test the *in vivo* activity of the monoamine oxidase variants, we added exogenous tyramine (or used a background strain expressing TYDC2) and performed metabolite analysis of the growth media. In samples expressing monoamine oxidase activities and supplemented with 1 mM tyramine, we used LC-UV to look for peaks corresponding to 4-HPA along with 4-hydroxyphenylacetic acid and 4-hydroxyphenylethanol (Fig 3.8c and Fig 3.7a). However, the major difference between these spectra was in the neighborhood of 6 min rather than the later elution times of the expected end products of known 4-HPA utilization pathways. The nature of these metabolites is unclear as no major ion is predominant in these peaks. The same strains grown in the absence of tyramine showed similar increases in this region, indicating that the monoamine oxidases may act on other natural metabolites as well. These *in vivo* assays also make it unclear whether the monoamine oxidase enzymes accept tyramine as a substrate. *In vitro* assays were performed using protein lysates from *E. coli* cells overexpressing the native MaoA. Although we could not detect 4-HPA from the MaoA reaction, we were able to successfully couple this product to the NCS reaction to produce

norcoclaurine *in vitro* (Fig. 3.8d). This provides evidence that the bacterial monoamine oxidase is capable of producing 4-HPA but it is currently unclear whether *in vivo* conditions in yeast are conducive to this reaction.

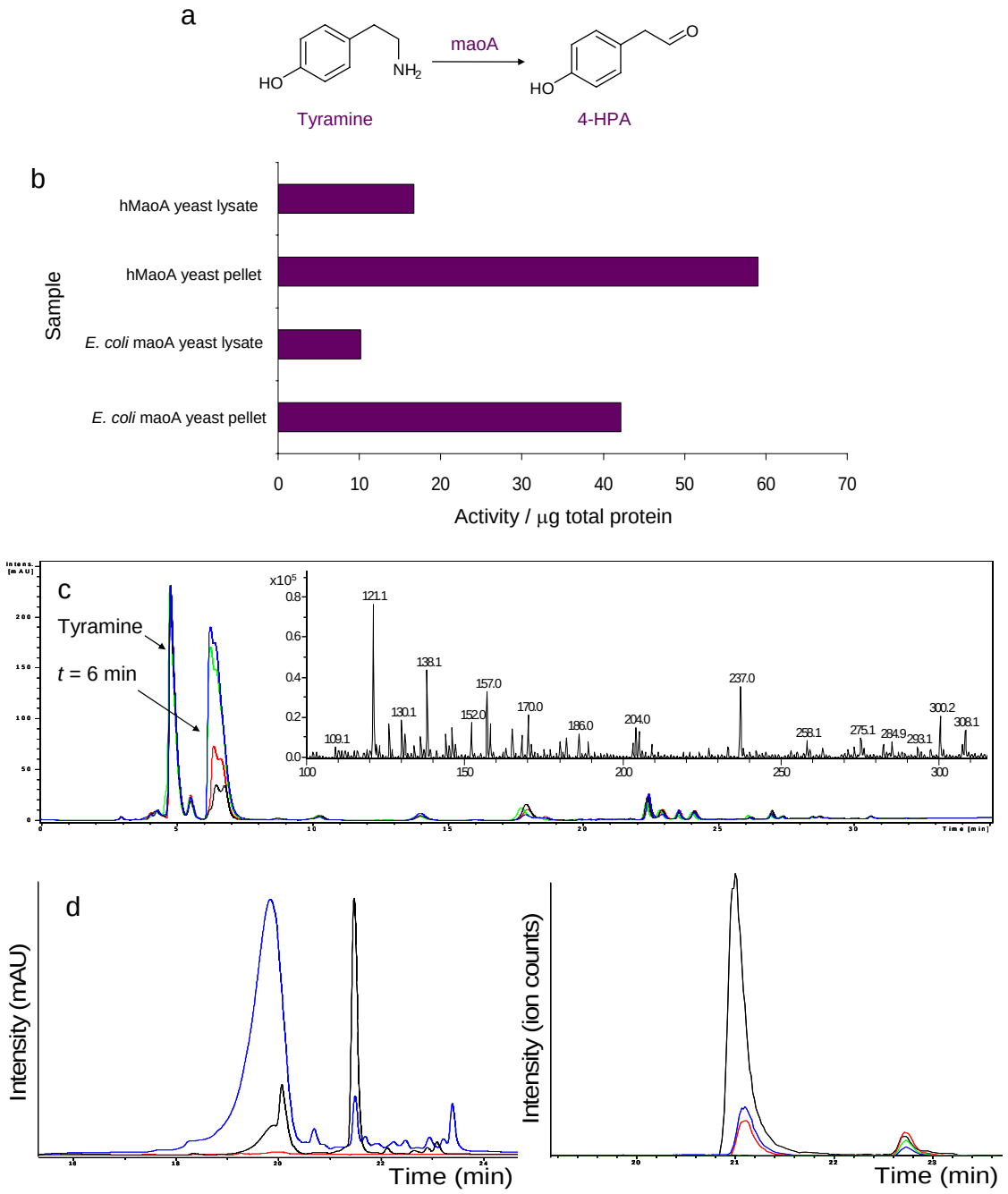

Fig. 3.8 Monoamine oxidase enzyme assays. **(a)** Pathway for the conversion of tyramine to 4-HPA using a monoamine oxidase activity. **(b)** Results of H_2O_2 assay on yeast cell lysates and lysed cell pellets. The majority of monoamine oxidase activity is found in the

cell pellet consistent with Western blotting experiments which indicate that the majority of the monoamine oxidase protein co-localizes with the cell debris upon lysis with Y-PER. **(c)** LC-UV analysis of the growth media of yeast strains supplemented with 1 mM tyramine. Negative control (no monoamine oxidase) = black; *E. coli* maoA = red; hMaoA = green; *M. luteus* maoA = blue. The inset ion chromatogram is representative of the enlarged peak at ~6 min seen in strains expressing the monoamine oxidase; no major ion is dominant. **(d)** Left: LC-UV analysis (276 nm) of *E. coli* maoA *in vitro* reaction (red), tyramine oxidase *in vitro* reaction (positive control; blue) and 4-HPA (black). Right: Extracted ion chromatograms (*m/z* = 272) of NCS *in vitro* reactions with *E. coli* maoA reaction product (red), tyramine oxidase reaction product (blue), authentic 4-HPA (black), and no 4-HPA (green).

Each of these monoamine oxidase variants from bacteria and human sources are reported to accept tyramine and dopamine along with other similar substrates. This means that these enzymes can produce 3,4-DHPA in addition to 4-HPA since tyramine and dopamine are both potentially available intermediates in our system. It has been reported previously that dopamine and its oxidized product 3,4-DHPA can spontaneously condense to form norlaudanosoline (Fig. 3.9a)[51]. This is also a potentially useful molecule as it differs from the natural intermediate norcoclaurine by only a 3'-hydroxyl group. Although the formation of norlaudanosoline from dopamine was recently reported to occur in *E. coli* supplemented with 5 mM dopamine[50], we found that in our strains up to 100 mM exogenous dopamine was required to detect accumulation of norlaudanosoline in the growth media. We also found that the human MAO-A is the preferred variant for this reaction as expected according to its biological function (Fig. 3.9b).

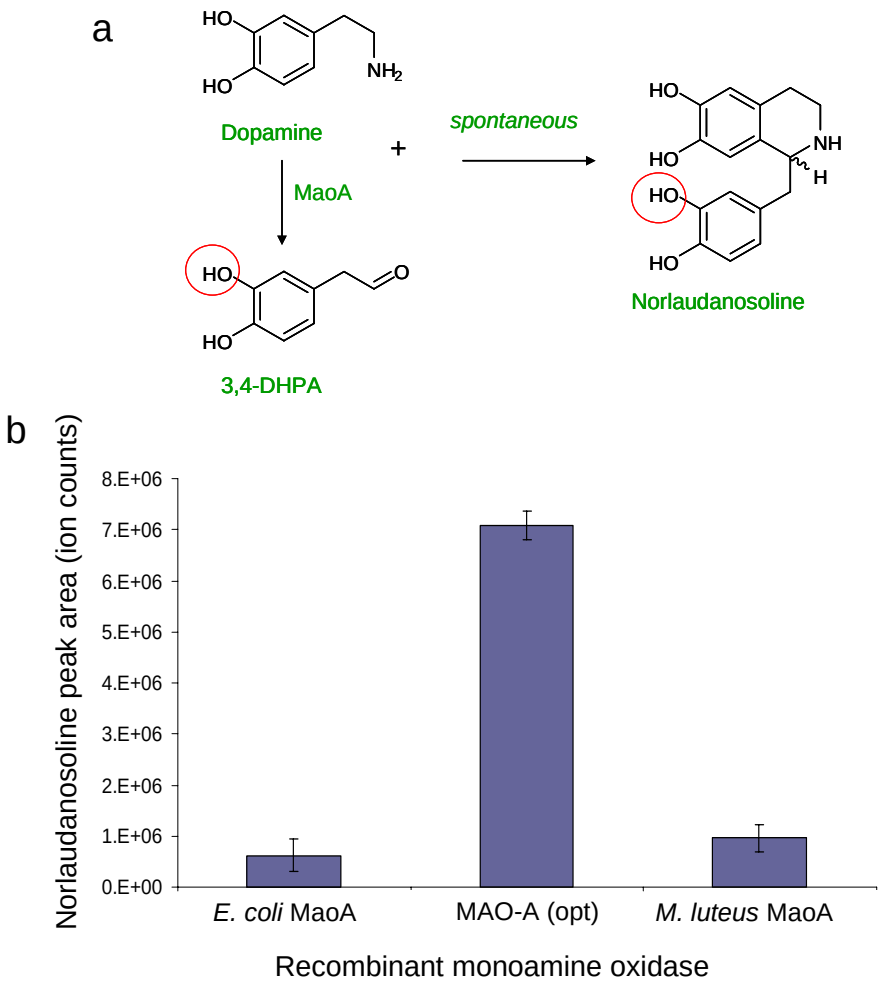

Fig. 3.9. Production of norlaudanosoline from dopamine. **(a)** Pathway for dopamine conversion to 3,4-DHPA and norlaudanosoline. The only difference between norcoclaurine and norlaudanosoline is the presence of the 3'-hydroxyl group circled in red. **(b)** Comparison of norlaudanosoline production between strains expressing the *E. coli* MaoA, the human MAO-A optimized for yeast, and the *M. luteus* MaoA supplemented with 0.1 M dopamine.

Although we were able to produce detectable levels of norlaudanosoline, it was still unclear why this reaction was so inefficient in our yeast hosts, requiring 20x more dopamine than reported for *E. coli*[50]. Possible reasons include transport, spontaneous oxidation of dopamine at low pH, and degradation of the 3,4-DHPA intermediate by endogenous enzymes. In an attempt to facilitate dopamine uptake, we constructed strains to overexpress a mutant form of the general amino acid permease ($Gap1^{K9K16}$)[52] and

observed a 6 to 7-fold increase in norlaudanosoline production (Fig. 3.10a). We also tested single *ADH* knockouts expressing MAO-A and observed a ~30-fold increase in norlaudanosoline production from 100 mM dopamine in *adh2Δ*, *adh5Δ*, and *adh6Δ* strains (Fig. 3.10b). While we did observe increases in norlaudanosoline accumulation of ~15-fold in *ald2Δ* and *ald3Δ* strains, the results indicated that that 3,4-DHPA is preferentially oxidized to the alcohol in standard yeast media. A combinatorial knockout of *ADH2*, *ADH5, ADH6, ALD2,* and *ALD3* alcohol and aldehyde dehydrogenase enzymes is expected to show additive effects. Future work includes testing of combinatorial *ADH* and *ALD* knockout strains for an increase in the flux of 4-HPA and 3,4-DHPA through our recombinant pathway.

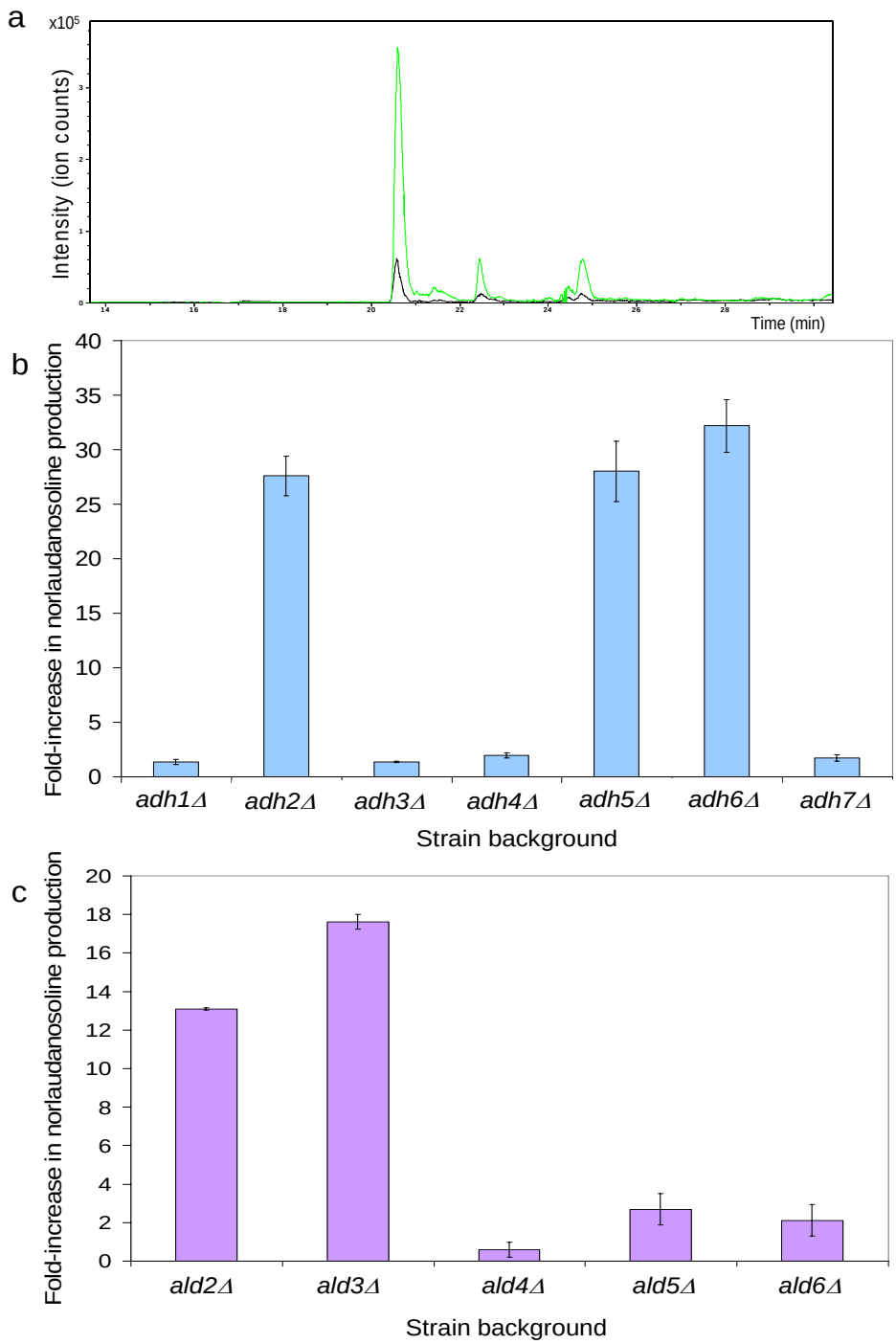

Fig. 3.10. Strains with increased norlaudanosoline accumulation. **(a)** Extracted ion chromatogram of norlaudanosoline (*m/z* = 288) produced from 1 mM dopamine in yeast strains expressing MAO-A and Gap1p^{K9K16} (green) and MAO-A only (black). The peak at 20.7 min is the correct norlaudanosoline product. **(b)** Norlaudanosoline production from 100 mM dopamine in *ADH1-7* and **(c)** *ALD2-6* single knockout strain backgrounds expressing MAO-A normalized to the same background strain expressing MAO-A with no deletions.

An alternative pathway to 4-HPA uses endogenous yeast genes *ARO8/9* and *ARO10* involved in the biosynthesis and degradation of tyrosine (Fig. 3.11). The *ARO8* and *ARO9* genes are analogous aromatic amino acid transaminase activities. Aro8p, classified as a type I aminotransferase, produces L-glutamate from 2-oxoglutarate as a by-product whereas Aro9p, a type II aminotransferase, produces L-alanine from pyruvate[53]. The *ARO10* gene product is a decarboxylase enzyme implicated in the degradation of aromatic and branched chain amino acids for the production of fusel alcohols via the Erhlich pathway.

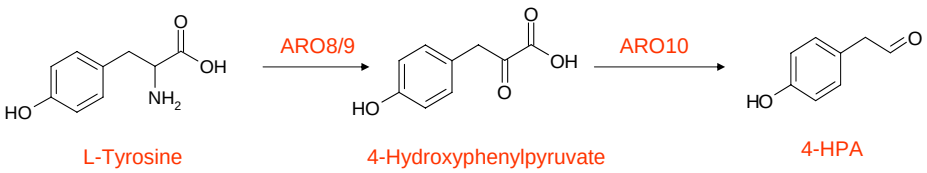

Fig. 3.11. Pathway for the production of 4-HPA from tyrosine using the endogenous yeast genes *ARO8/9* and *ARO10*.

Since the *ARO* genes are native to yeast, they are an obvious choice for this activity. However, these genes are also subject to endogenous regulation designed to prevent utilization of inferior nitrogen sources. For example, Aro9p expression levels are more than 10-fold higher when grown on urea versus ammonia, a superior nitrogen source, with similar transcriptional regulation expected for Aro10p[54]. Transcriptional regulation alone is simple to overcome by expressing the gene behind a promoter that is constitutive and/or active under the desired growth conditions. However, experimental results using strains with constitutive expression of Aro10p indicate that this protein is subject to post-translational regulation and/or requires a second protein for activity[55]. As the details of this regulation are still unknown, we expect Aro10p to show low activity in

cultures grown on glucose and ammonia. With this in mind, we made plasmid-based constructs to constitutively express *ARO8*, *ARO9* and *ARO10*. We transformed an empty vector control, a plasmid expressing *ARO8* or *ARO9* only, and a plasmid expressing both *ARO9* and *ARO10* and examined the growth media for the formation of UV peaks corresponding to 4-HPA and its metabolites in standard synthetic complete yeast drop-out media (Fig. 3.12). In strains expressing only *ARO8* or *ARO9*, we observed an increase in the peak identified as 4-hydroxyphenylpyruvate, and in strains expressing *ARO9* and *ARO10*, we observed this same peak plus an additional peak corresponding to tyrosol. No peaks corresponding to 4-HPA were observed. These results suggest that overexpression of *ARO8/ARO9* and *ARO10* can convert tyrosine to 4-HPA, and moreover, that the 4-HPA is efficiently converted to tyrosol under standard glucose-grown conditions.

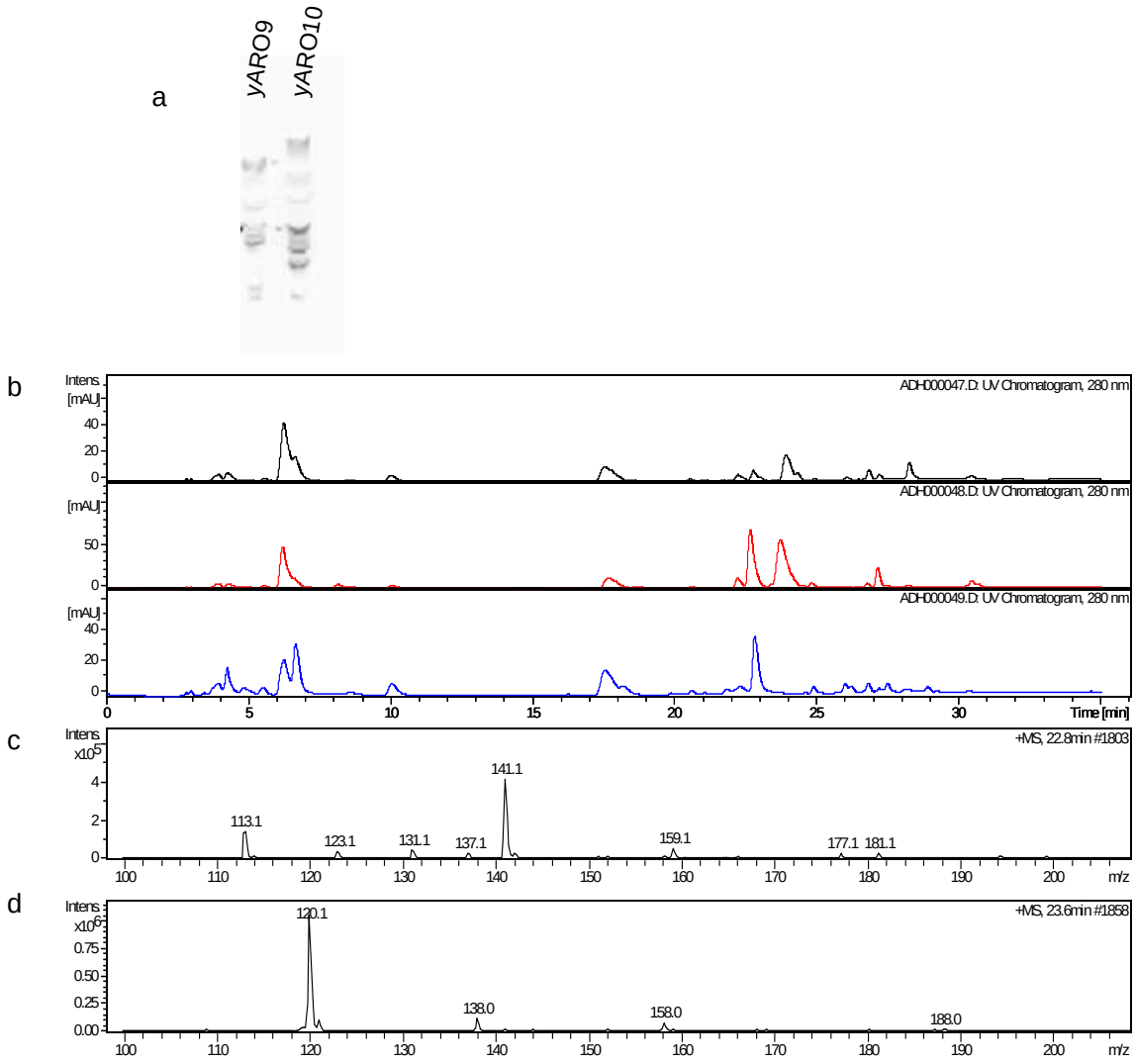

Fig. 3.12. Analysis of yeast strains overexpressing the *ARO* genes. **(a)** Western blotting using C-terminal V5 epitope tags indicate extensive proteolytic processing of Aro9p and Aro10p under glucose-grown conditions. **(b)** LC-UV chromatograms of the growth media of yeast strains constitutively expressing *ARO* genes. Negative control lacking an enzyme coding sequence (black), *ARO9* and *ARO10* (red), and *ARO9* only (blue). **(c)** Mass spectrometer data for the peak at 22.8 min identified as 4-hydroxyphenylpyruvate with the major ion *m/z* = 181. **(d)** Mass spectrometer data for the peak at 23.6 min identified as tyrosol with characteristic ions *m/z* = 138 and *m/z* = 120.

We tested a construct overexpressing Aro9p and Aro10p in the *ADH* and *ALD* knockout strains hoping to observe decreased conversion to tyrosol and the possible emergence of a peak corresponding to 4-HPA. While we did observe a slight increase in

4-HPA production in many of the knockouts, we also observed larger increases in tyrosol and 4-hydroxyphenylacetic acid. This is surprising and likely a consequence of the cells adjusting to overexpression of the ARO genes. It is unclear whether combinatorial knockouts will show more promising results.

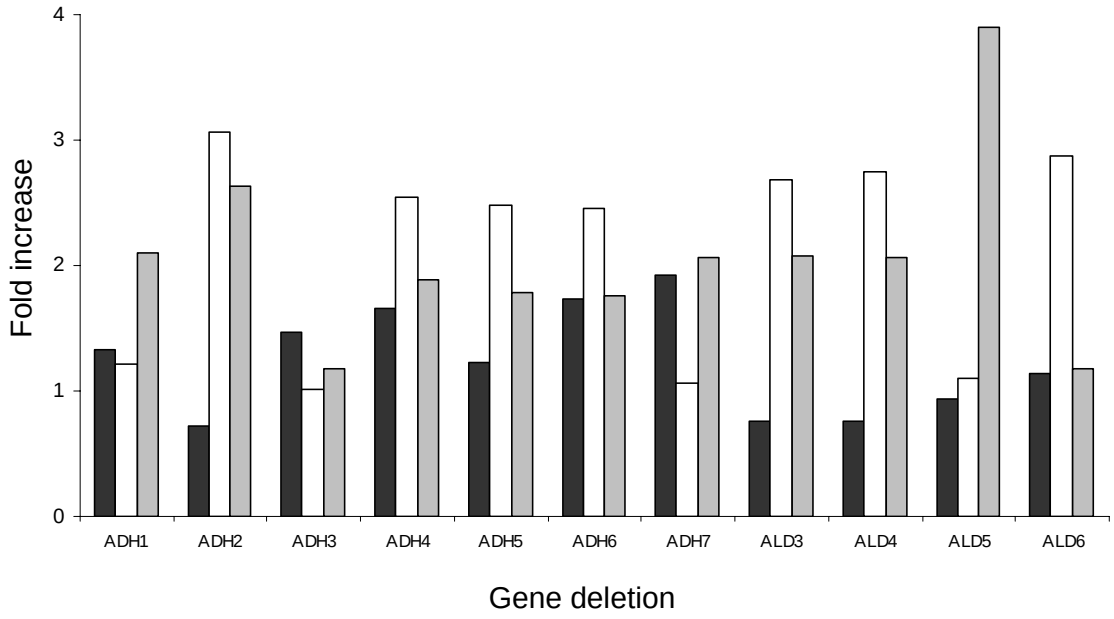

Fig. 3.13. Changes in 4-HPA, tyrosol, and 4-hydroxyphenylacetic acid production in knockout strains overexpressing Aro9p and Aro10p. Production of 4-HPA (black), tyrosol (white), and 4-hydroxyphenylacetic acid (grey) are shown for each knockout strain background; the area of each UV chromatogram peak is normalized to the control strain also expressing Aro9p and Aro10p with no gene deletions.

3.2.4. Production of norcoclaurine and norlaudanosoline

The end goal of the aforementioned engineered yeast strains is to produce a sufficient amount of dopamine and 4-HPA (or 3,4-DHPA) to be incorporated into the BIA backbone molecules norcoclaurine and/or norlaudanosoline. Both products are possible with the same combination of enzymes if a monoamine oxidase activity is used and both tyramine and dopamine substrates are present. However, assuming the *ARO*

genes will produce only 4-HPA from tyrosine and no other aldehydes that can react with dopamine, we should accumulate only norcoclaurine in engineered strains using this alternative pathway (Fig. 3.14)

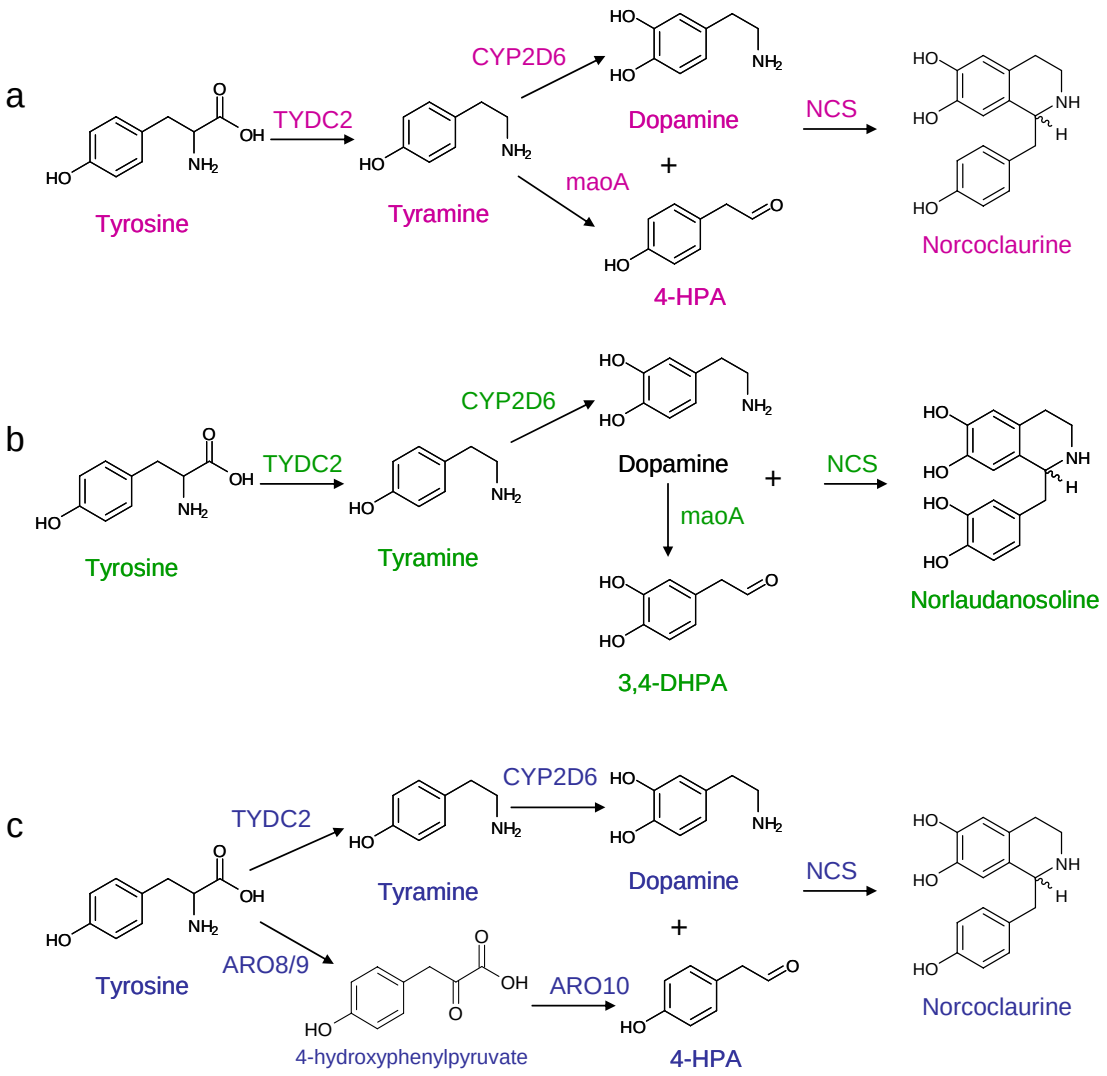

Fig. 3.14. Pathways for norcoclaurine and norlaudanosoline production. The NCS activity catalyzing the final step is optional as this condensation reaction occurs spontaneously *in vivo*. **(a)** Production of norcoclaurine using TYDC2, CYP2D6, and maoA. **(b)** Production of norlaudanosoline using the same set of enzymes as shown in (a). **(c)** Production of norcoclaurine using TYDC2 and CYP2D6 to produce dopamine and the yeast *ARO* genes to produce 4-HPA.

In plants, the enzyme norcoclaurine synthase (NCS) catalyzes the reaction between dopamine and 4-HPA. NCS has been cloned and characterized from *T. flavum*[56] and *C. japonica*[57]; however, the homologous PR10 proteins from *P. somniferum* are not catalytically active. Mechanistic studies on the *T. flavum* and *C. japonica* NCS variants show that these proteins from two different families are capable of catalyzing the same reaction *in vitro* although it is unclear what role NCS plays in the native hosts.

We obtained the *T. flavum* NCS variant to test in our engineered yeast strains. Previous characterization of the *T. flavum* NCS showed that removal of the N-terminal signal sequence by making a Δ10 or Δ19 truncation facilitated soluble expression in a recombinant host[56]; however, we were also able to observe expression of the full-length NCS in our strains (Fig. 3.15a). We tested each variant *in vitro* and *in vivo* with exogenous dopamine and 4-HPA. Not only did we not observe differences between the NCS variants, but we found that negative controls lacking an NCS sequence produced similar levels of norcoclaurine. We observed this same product in *in vitro* reactions containing wild-type yeast lysates but not when *E. coli* lysates were used. All *in vivo* and *in vitro* products had the same elution time and the correct mass fragmentation pattern (Fig. 3.15b)[56]. Our finding that NCS is not required for the formation of the BIA backbone is in agreement with other studies using heterologous hosts[50].

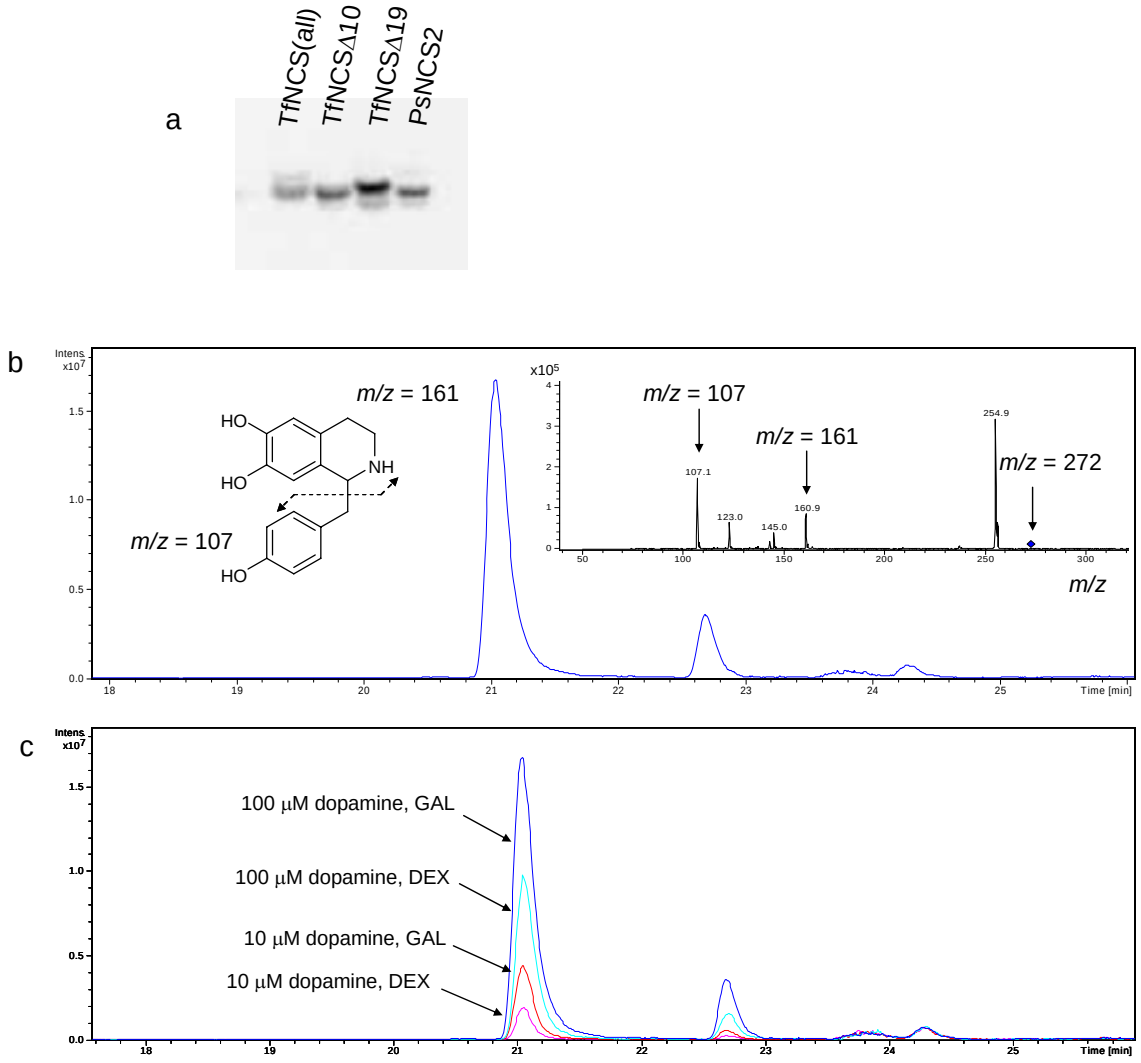

Fig. 3.15. Expression of NCS and production of norcoclaurine. **(a)** Western blot showing expression of V5-tagged proteins—*T. flavum* NCS (entire sequence), NCSΔ10, and NCSΔ19. The *P. somniferum* NCS2 variant is also shown but not discussed as subsequent reports indicate it is not catalytically active[6]. **(b)** Production of norcoclaurine *in vivo* by feeding dopamine and 4-HPA. The extracted ion chromatogram of *m/z* = 272 is shown in blue, with the inset showing the correct fragmentation pattern for this product eluting at 21 min; the second peak at 22.7 min also showed the correct fragmentation pattern and was consistent in all *in vivo* and *in vitro* experiments. **(c)** Norcoclaurine production by feeding 4-HPA and limiting amounts of dopamine. NCS was expressed from a GAL-inducible promoter to demonstrate that the enzyme assists this reaction when one (or both) substrates is limiting. Extracted ion chromatograms for norcoclaurine (*m/z* = 272) are shown; magenta = 10 μM dopamine grown in dextrose; red = 10 μM dopamine

grown in galactose; cyan = 100 μM dopamine grown in dextrose; blue = 100 μM dopamine grown in galactose.

We also performed experiments titrating dopamine in a strain with the TfNCSΔ10 expressed from the GAL1-10 promoter. The results show that expression of NCS increases production of norcoclaurine when one or both substrates are limiting (Fig. 3.15c). In contrast to this result, however, we found that expression of NCS hindered norlaudanosoline production. We fed 100 mM dopamine to strains expressing MAO-A alone or with co-expression of TfNCSΔ10 and observed much lower norlaudanosoline production in strains co-expressing TfNCSΔ10 (Fig. 3.16). We also fused matching C-terminal leucine zippers[58] to each enzyme to facilitate co-localization of the 3,4-DHPA and NCS enzyme for a more efficient reaction and to prevent degradation of the acetaldehyde intermediate. Substantially lower norlaudanosoline production was also observed in this strain. It is not surprising that NCS does not facilitate this reaction since 3,4-DHPA is not the true substrate. However, the mechanism by which the enzyme actually interferes with norlaudanosoline production is unclear. Perhaps the substrates can bind to the protein but not react in the active site due to presence of the additional hydroxyl group.

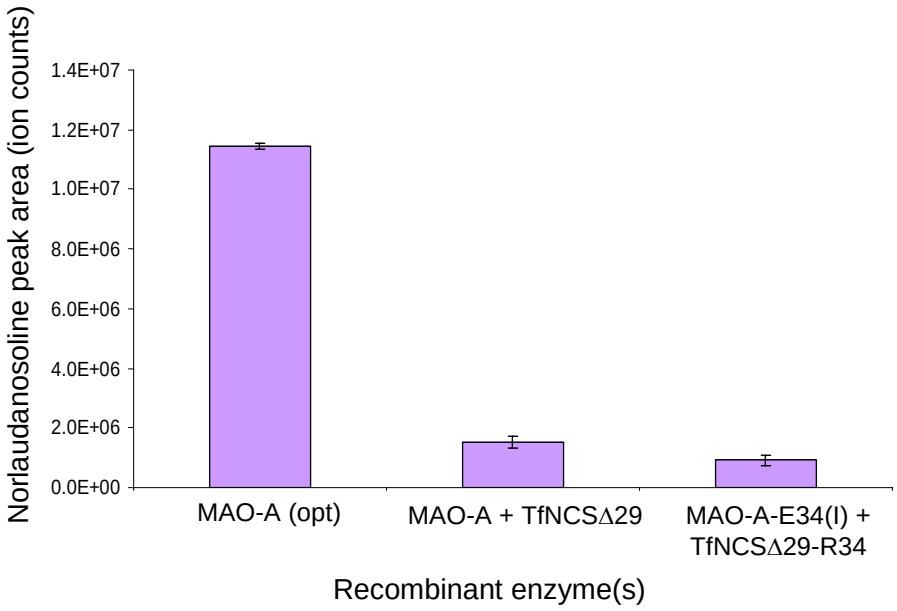

Fig. 3.16. Comparison of norlaudanosoline production with NCS. Norlaudanosoline production as measured by the extracted ion chromatogram area of strains expressing the human MAO-A optimized for yeast with or without the *T. flavum* NCSΔ29 and with C-terminal leucine zippers to co-localize the hMaoA and the *T. flavum* NCSΔ29.

We also tested production of norcoclaurine in our *ADH* and *ALD* knockout strains expressing ARO9 and ARO10. For these experiments, we also had to feed a large excess of dopamine (100 mM) to see production of norcoclaurine. While we were able to observe increases in norcoclaurine production in several of the knockout strains, the results were not as dramatic as those observed for norlaudanosoline, with a maximum increase of ~3-fold compared to ~35-fold for norlaudanosoline. This is consistent with observations of 4-HPA, tyrosol, and 4-hydroxyphenylacetic acid production which suggest that the 4-HPA intermediate is otherwise diverted when only one of these enzymes is deleted. Since 4-HPA is a natural intermediate, it is also logical that multiple endogenous enzymes are capable of converting this substrate while fewer may act on 3,4-DHPA and/or have lower activity on this acetaldehyde. It is unclear from these results

whether combinatorial knockouts will have additive effects or how many deletions are required to prevent 4-HPA degradation. Once combinatorial knockouts are constructed, we can test strains co-expressing Gap1^{K9K16} to improve dopamine transport. Ultimately, however, we would like to incorporate enzymes for *in vivo* dopamine production in these strains as well. Expression of NCS is also expected to enhance norcoclaurine production when substrate concentrations are low.

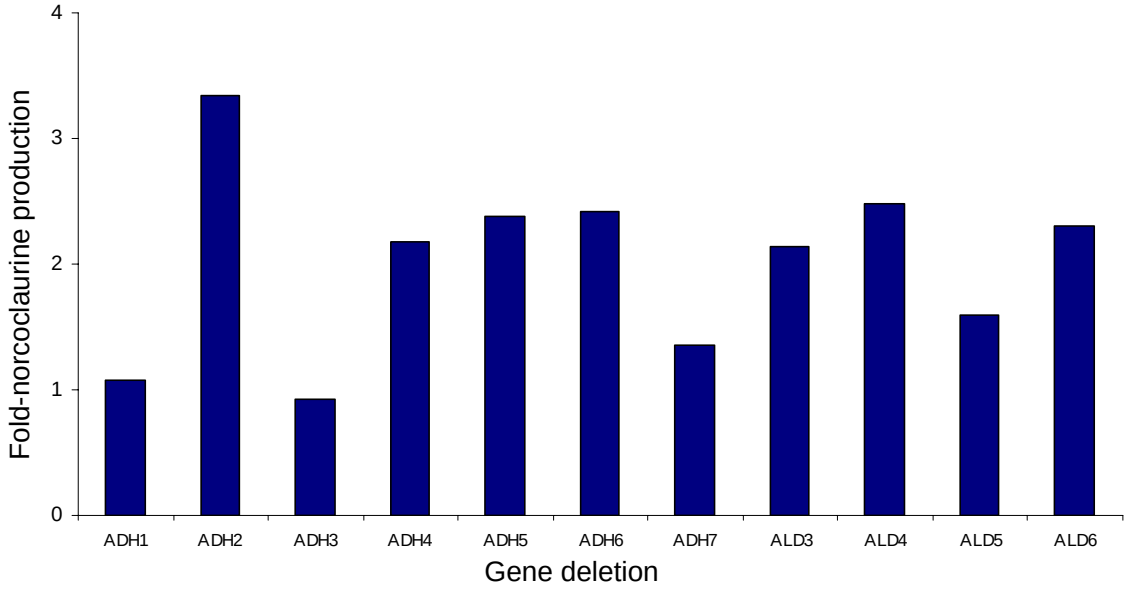

Fig. 3.17. Norcoclaurine production in *ADH* and *ALD* knockout strains. The fold increase in norlaudanosoline production from strains expressing Aro9p and Aro10p supplemented with 100 mM dopamine is normalized to the control strain with no deletions. Norcoclaurine is measured as the area of the extracted ion chromatogram peak (*m/z* = 272) with an elution time of 21.2 min.

Our results show that the production of norcoclaurine and norlaudanosoline occur readily in our yeasts hosts when sufficient precursors are available. The expression of NCS may lead to higher yields of norcoclaurine but may actually inhibit norlaudanosoline production. Expression of NCS may be one way to direct production of either norcoclaurine or norlaudanosoline as an alternative to using the *ARO* genes for

production of only the 4-HPA intermediate. It is also noteworthy that other variants such as the *Coptis japonica* NCS may have different specificities. The *C. japonica* NCS was reported to have a different mechanism[57], and although it also failed to enhance norlaudanosoline synthesis in a microbial host, it reportedly did not inhibit this reaction[50].

3.3. Discussion

We have identified several recombinant and endogenous yeast enzymes capable of performing the reactions to produce the BIA backbone molecules norcoclaurine and norlaudanosoline from tyrosine. We have constructed yeast strains to test these pathways and made several efforts to optimize production of the precursor molecules. However, we have not yet reached levels of dopamine required for the total biosynthesis of norcoclaurine and/or norlaudanosoline *in vivo*. While we have demonstrated production of tyramine and dopamine, we believe that dopamine is still limiting based on experiments showing production of BIA molecules upon exogenous addition of dopamine.

For the production of norlaudanosoline, which is not the natural intermediate but useful for synthetic pathways, we were able to demonstrate production by feeding dopamine and expressing only the human MAO-A. However, this remains an extremely inefficient process even with improvements in intracellular transport and partial elimination of a competing pathway. Again, *in vivo* dopamine production was not sufficient to be converted to 3,4-DHPA and norlaudanosoline. These negative results may be due, at least in part, to the autooxidation of dopamine and the instability of the acetaldehyde intermediate. Similarly, we were able to demonstrate production of

norcoclaurine by feeding dopamine and expressing Aro9p and Aro10p. Production was significantly enhanced in several *ADH* and *ALD* knockout backgrounds. From our best strains containing only one gene deletion and not co-expressing Gap1p^{K9K16}, we are able to produce ~ 10 mg l^{-1} norcoclaurine or norlaudanosoline from 100 mM dopamine.

Much work remains to optimize the individual pathways for norcoclaurine and norlaudanosoline production. This may require the exploration of other enzymatic activities or protein engineering/evolution, particularly to increase the activity of CYP2D6 and/or AbPPO2. The construction of combinatorial knockouts and possibly additional strain engineering is likely required to direct the flux of 4-HPA and 3,4-DHPA towards BIA production by blocking endogenous degradation pathways. In addition, advanced engineering strategies such as building protein scaffolds may be employed to increase local concentrations of these intermediates and facilitate metabolite channeling between enzymes.

3.4. Materials and Methods

3.4.1. Plasmid and yeast strain construction

We obtained restriction enzymes, T4 DNA ligase, and other cloning enzymes from New England Biolabs. We performed polymerase chain reaction (PCR) amplifications using Expand High Fidelity PCR System (Roche). Oligonucleotide synthesis was performed by Integrated DNA Technologies. A list of selected plasmids and yeast strains is provided (Table 3.1).

We used standard molecular biology techniques to construct the BIA expression vectors[59]. BIA expression constructs contained the 2μ high-copy yeast origin of

replication along with appropriate yeast selection markers and ampicillin resistance. Recombinant enzymes were expressed from the yeast TEF1 promoter and flanked by a CYC1 terminator sequence. We constructed shuttle vectors for subcloning of 1 or 2 cDNA sequences in this fashion. The *hCYP2D6* cDNA was provided by F. Peter Guengerich (Vanderbilt University) as pCW/DB6[60] and the yeast codon-optimized version of this gene was synthesized by DNA 2.0. We PCR-amplified the endogenous yeast P450 reductase gene (*CPR1*) from W303 genomic DNA and the *Homo sapiens CPR1* gene from pH2E1red[61].

We transformed ligation reactions into an electrocompetent *E. coli* strain, DH10B (Invitrogen; F-*mcr*A Δ(*mrr-hsd*RMS-*mcr*BC) ϕ80d*lac*ZΔM15 Δ*lac*X74 *deo*R *rec*A1 *end*A1 *ara*D139 Δ (*ara, leu*)7697 *gal*U *gal*K λ-*rps*L *nup*G), using a Gene Pulser Xcell System (BioRAD) according to the manufacturer's instructions. We conducted plasmid isolation using the Wizard Plus SV Minipreps DNA purification system (Promega) according to the manufacturer's instructions. Subcloning was confirmed by restriction analysis and sequence verification (Laragen, Inc.). We transformed plasmids into the appropriate *S. cerevisiae* strains using a standard lithium acetate protocol[62]. All yeast strains used in this work were based on the haploid yeast strain W303α (MATα *his3-11,15 trp1-1 leu2-3 ura3-1 ade2-1*)[63]. *E. coli* cells were grown on Luria-Bertani media (BD Diagnostics) with 100 μg/ml ampicillin (EMD Chemicals) for plasmid maintenance, and *S. cerevisiae* cells were grown in synthetic complete media (BD Diagnostics) supplemented with the appropriate dropout solution for plasmid maintenance (Calbiochem).

Table 3.1. Plasmids and yeast strains.

Plasmids	
pCS138	P_{TEF1}-*GAP1*^{K9K16}
pCS221	P_{TEF1}-*TYDC2*
pCS250	P_{TEF1}-*TfNCSΔ10*
pCS251	P_{TEF1}-*AbPPO2*
pCS283	P_{TEF1}-*TYDC2* , P_{TEF1}-*maoA*
pCS330	P_{TEF1}-*TYDC2* , P_{TEF1}-*yCYP2D6*
pCS405	$P_{GAL1-10}$-*TfNCSΔ10(V5-HIS tag)*
pCS637	P_{TEF1}-*yARO10*
pCS689	P_{TEF1}-*yARO9*, P_{TEF1}-*yARO10*
pCS785	P_{TEF1}-*maoA(V5-HIS tag)*
pCS886	P_{TEF1}-*TyrH* , P_{TEF1}-*hGTPCHI*
pCS887	P_{TEF1}-*hTH2* , P_{TEF1}-*hGTPCHI*
pCS1050	P_{TEF1}-*hMaoAopt(V5-HIS tag)*
pCS1227	P_{TEF1}-*yARO8*
pCS1480	P_{TEF6}-*yCYP2D6*
pCS1482	P_{TEF1}-*hMaoAopt-E34(I)* , P_{TEF1}-*TfNCSΔ29-R34*
pCS1537	P_{TEF1}-*MlmaoAopt*
pCS1546	P_{TEF1}-*TYDC1*
pCS1565	P_{TEF6}-*yCYP2D6:yCPRΔ33 fusion*
pCS1591	P_{TEF1}-*hMaoAopt* , P_{TEF1}-*TfNCSΔ29*

Yeast strains	**Plasmid(s)**	**Integrated constructs**	**Plasmid-based constructs**
CSY194		$P_{GAL1-10}$-*yCPR1*	
CSY195		$P_{GAL1-10}$-*AtATR1*	
CSY88	pCS221, pCS251		P_{TEF1}-*TYDC2*, P_{TEF1}-*AbPPO2*
CSY151		wild-type	
CSY152		*ald2Δ*	
CSY153		*ald3Δ*	
CSY154		*ald4Δ*	
CSY155		*ald5Δ*	
CSY156		*ald6Δ*	
CSY417		*adh1Δ*	
CSY418		*adh2Δ*	
CSY419		*adh3Δ*	
CSY420		*adh4Δ*	
CSY421		*adh5Δ*	
CSY422		*adh6Δ*	
CSY423		*adh7Δ*	

3.4.2. Analysis of metabolite production

We evaluated BIA metabolite levels by LC-MS/MS analysis of cell extracts and growth media. At appropriate time points, aliquots of yeast cultures were centrifuged to recover cells as pellets and allow collection of the growth media. We analyzed the growth media or an appropriate dilution directly by LC-MS/MS. Samples were run on an Agilent ZORBAX SB-Aq 3 x 250 mm, 5 μm column with 0.1% acetic acid as solvent A and methanol as solvent B. We used a gradient elution to separate the metabolites of interest as follows: 0-10 min at 100% A, 10-30 min 0-90% B, 30-35 min 90-0% B, followed by a

5 min equilibration at 100% A between samples. Following LC separation, metabolites were injected into an Agilent 6320 ion trap MSD for detection and identification. We verified chromatogram data through at least three independent experiments and from multiple strains where appropriate. Quantification of metabolites was based on the integrated area of the extracted ion chromatogram peaks[64] calculated using DataAnalysis for 6300 Series Ion Trap LC/MS Version 3.4 (Bruker Daltonik GmbH) and reported as the mean ± s.d. When appropriate, we normalized the measured levels to a metabolite peak of known concentration in the growth media.

3.4.3. Analysis of protein levels through Western blotting

We constructed plasmids for Western blotting experiments by cloning the C-terminal epitope tag(s) from pYES-NT/A (Invitrogen) into our standard TEF1 expression vector followed by subcloning of the enzyme of interest. For the AbPPO2 construct with the N-terminal tag, we cloned this sequence into the original GAL-inducible pYES-NT/A vector and detected with the Anti-His G-HRP antibody. We transformed individual plasmids into wild-type yeast cells using a standard lithium acetate protocol. Overnight cultures were grown and backdiluted 1:100 into 100 ml cultures. Cells were grown to OD_{600} ~1.5 and pelleted by centrifugation. The media was removed and cells were washed in 1 ml PBS, pelleted, and resuspended in 0.5 ml Y-PER plus HALT protease inhibitor (Pierce). Cells were vortexed for ~20 min and the lysate separated by centrifugation. We estimated total protein using the Coomassie Plus Protein Assay Reagent (Pierce) and loaded ~50 μg of each sample onto a protein gel. We used NuPage 4-12% Bis-Tris gels with MES running buffer and transfer buffer according to the manufacturer's instructions (Invitrogen). Proteins were blotted onto a nitrocellulose

membrane (Whatman) using a semi-dry transfer cell (Bio-Rad) for 25 min at 25 V. We incubated the membrane with the Anti-V5 HRP antibody (Invitrogen) according to the manufacturer's instructions (Invitrogen) with 5% BSA as the blocking agent. Proteins were detected with the West Pico Super Signal Detection kit (Pierce) and imaged on a ChemiDoc XRS system (Bio-Rad).

3.4.4. Monoamine oxidase and NCS in vitro assays

For the monoamine oxidase H_2O_2 assays, yeast cells were grown in 50-100 ml cultures and lysed with 0.5 ml Y-PER plus HALT protease inhibitor (Pierce). Cell pellets were resuspended in 0.5 ml PBS, and total protein for each sample was estimated using the Coomassie Plus Protein Assay Reagent (Pierce) to normalize activity. Standard curves were generated and plate-based assays performed using the Fluoro H_2O_2 kit (Cell Technology, Inc.) according to the manufacturer's instructions. The activity was compared to a negative control lacking a monoamine oxidase sequence (this value was subtracted from the data presented).

For the monoamine oxidase *in vitro* reactions, *E. coli* cells were used to express the recombinant proteins since maoA can be recovered in the soluble lysate of bacterial samples whereas most protein associates with the cell pellet in yeast. *E. coli* cells expressing maoA or NCS from the P_{trc} promoter were induced with 1 mM IPTG and grown for ~12 hr in 10 ml cultures. The cells were harvested by centrifugation and lysed with B-PER plus HALT (Pierce). Soluble lysates were desalted using NAP columns and resuspended in the appropriate reaction buffer. For maoA assays, the reaction consisted of 0.1 M potassium phosphate, pH 7.0, 10 mM tyramine, and 100 µl maoA lysate in a

total volume of 1 ml incubated at 37ºC for 1 hr. For NCS assays, the reaction consisted of 0.1 M Tris-HCL, pH 7.5, 10 mM dopamine, 10 µl maoA reaction, and 50 µl NCS lysate in a total volume of 100 µl incubated at 37ºC for 1.5 hr. For the maoA reaction, purified tyramine oxidase from *Arthrobacter sp.* (Sigma) was used as a positive control in the described maoA reaction mixture and also under the recommended conditions.